# Making Algebraic Parameter Estimation Practical for Noisy Data via Gaussian Process Regression

Oren Bassik[*]        Alexander Demin[†]        Alexey Ovchinnikov[‡]

### Abstract

Parameter estimation for ordinary differential equation (ODE) models is a critical task often hindered by noisy data and the limitations of traditional optimization methods. The differential-algebraic approach offers theoretical advantages, such as eliminating the need for initial parameter guesses, and finding all global solutions without getting stuck in local minima. The algebraic approach has been historically hampered by its sensitivity to measurement noise. In this work, we resolve this limitation by replacing the noise-sensitive derivative estimation step with a robust probabilistic framework based on Gaussian Process Regression (GPR). We demonstrate through a comprehensive benchmark across 550 datasets on 11 dynamical systems that our GPR-enhanced method is highly competitive with modern optimization techniques. When paired with a local refinement step, our method achieves the highest success rate (58.5%) for high-precision (1% error) tasks, making the powerful differential-algebraic method a practical and reliable tool for parameter estimation from real-world, noisy data.

## 1   Introduction

Parameter estimation for systems of ordinary differential equations (ODEs) is a fundamental challenge in nearly every field of science and engineering. While ODE models are ubiquitous, their practical use requires precise values for unknown parameters that must be inferred from experimental data. The dominant paradigm for this task is nonlinear optimization, where parameter values are sought that minimize the discrepancy between a model's simulated output and observed measurements. These "shooting" methods require repeated numerical integration of the ODE system, often once per iteration per candidate parameter set, which can be computationally intensive. Furthermore, these methods are susceptible to well-known drawbacks: they often require carefully chosen initial guesses to avoid converging to non-optimal local minima, and they typically identify only a single parameter set, which is insufficient for systems where parameters are only locally identifiable.

An alternative, the differential-algebraic approach, offers a compelling solution to these challenges. By transforming the ODE system into a set of algebraic equations, this method can, in principle, find all valid parameter sets without requiring any initial guesses from the user. This is achieved by converting the problem into one of solving a multivariate polynomial system, for which robust numerical solvers exist that can find all solutions globally. This makes it a powerful tool for global analysis and for systems with complex parameter landscapes. However, this approach has a critical vulnerability: it relies on computing high-order derivatives of the observed output signals,

---

[*]CUNY Graduate Center, New York, NY, USA.

[†]HSE University, Moscow, Russia.

[‡]CUNY Queens College and CUNY Graduate Center, New York, NY, USA.

a process that is notoriously sensitive to measurement noise. This sensitivity has largely prevented the widespread adoption of algebraic methods for practical applications, where data is invariably corrupted by noise.

To address this challenge, we introduce a methodology that replaces the noise-sensitive derivative estimation step with a robust statistical framework: Gaussian Process Regression (GPR). While the foundational algebraic framework was presented in [3] and benchmarked on noise-free data, the central contribution of this paper is demonstrating that the integration of GPR makes the method practical for realistic, noisy measurements, a claim we validate with an extensive benchmark.

The main contributions of this paper are:

1. The introduction of Gaussian Process Regression into the differential-algebraic parameter estimation workflow, extending this powerful theoretical method to be robust for noisy experimental data.

2. A comprehensive benchmark of this GPR-enhanced method against modern local and global optimization techniques across a diverse suite of 11 ODE systems and multiple noise levels.

3. A detailed analysis of the trade-offs between precision, robustness, and speed, providing practical guidance on which method to choose based on application requirements.

## 2 Background

Our methodology builds upon two distinct areas of scientific computing: the theory of differential algebra for parameter estimation and the statistical framework of Gaussian Process Regression. This section provides the necessary background in both areas.

### 2.1 The Differential-Algebraic Approach to Parameter Estimation

The differential-algebraic approach transforms a parameter estimation problem for a system of differential equations into a problem of solving a system of algebraic equations. The key insight is that the parameters of an ODE system are intrinsically linked to the higher-order derivatives of its outputs. A detailed exposition of this method can be found in [3, Section 3].

Given an ODE system with rational functions $\mathbf{f}$ and $\mathbf{g}$:

$$\begin{cases} \mathbf{x}'(t) = \mathbf{f}(\mathbf{x}(t), \mathbf{p}) \\ \mathbf{y}(t) = \mathbf{g}(\mathbf{x}(t), \mathbf{p}) \end{cases} \tag{1}$$

where $\mathbf{x}$ are the states, $\mathbf{p}$ are the parameters, and $\mathbf{y}$ are the observable outputs, one can repeatedly differentiate the output equation $\mathbf{y}(t) = \mathbf{g}(\mathbf{x}(t), \mathbf{p})$ with respect to time. Each differentiation introduces higher-order derivatives of $\mathbf{y}$ on one side and replaces derivatives of $\mathbf{x}$ with expressions from the system dynamics on the other. This process systematically eliminates the state variables $\mathbf{x}$ and their derivatives, resulting in a system of equations that algebraically relate the parameters $\mathbf{p}$ to the outputs $\mathbf{y}$ and their time derivatives $(\mathbf{y}, \mathbf{y}', \mathbf{y}'', \dots)$.

At any specific time point $t_0$, this symbolic system can be made numerical. If one can provide numerical values for the derivatives of the outputs at $t_0$, i.e., $y(t_0), y'(t_0), y''(t_0), \dots$, the result is a multivariate polynomial system solely in the unknown parameters $\mathbf{p}$. This system can then be solved using numerical algebraic geometry techniques, such as homotopy continuation, to find all possible solutions for $\mathbf{p}$ that are consistent with the observed data at that instant.

The power of this method lies in its ability to convert a global, dynamic optimization problem into a local, algebraic one. However, its practical success hinges entirely on the ability to obtain accurate numerical estimates for the derivatives of $\mathbf{y}(t)$ from discrete, noisy measurements.

## 2.2 Gaussian Process Regression for Derivative Estimation

Traditional methods for obtaining derivatives from data, such as finite differences or interpolation via splines or rational functions, are highly sensitive to noise. Differentiation is a high-pass filter, meaning it amplifies high-frequency components of a signal—and measurement noise is predominantly high-frequency. This amplification can render derivative estimates unusable, causing the algebraic method to fail.

To overcome this, we turn to Gaussian Process Regression (GPR). GPR is a non-parametric, Bayesian approach to regression that is exceptionally well-suited for fitting noisy data and estimating derivatives. Instead of fitting a single function to the data, GPR defines a prior distribution over a space of functions and then updates this prior to a posterior distribution based on the observed data.
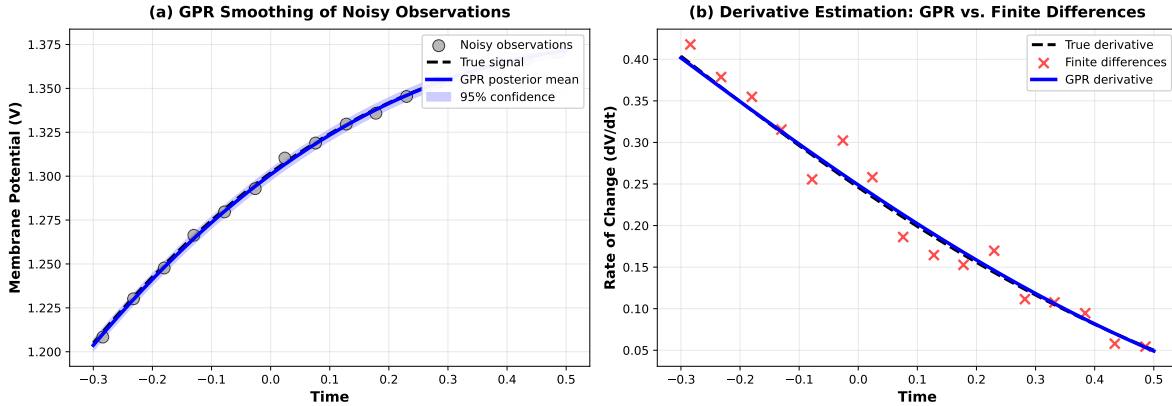


Figure 1: Demonstration of Gaussian Process Regression for derivative estimation using the FitzHugh-Nagumo system with 1% noise and 40 sparse observations. **(a)** GPR smoothing: Sparse noisy observations (gray points) are fit with a GPR model (blue line with 95% confidence interval). The GPR posterior mean accurately recovers the underlying smooth signal (black dashed line) despite significant measurement noise. **(b)** Derivative estimation comparison: Finite differences applied to the sparse noisy data (red X markers) versus the GPR-based derivative (blue line), compared against the true derivative (black dashed line). This demonstrates GPR's ability to produce stable, accurate derivative estimates even from noisy sparse data—the key enabler for the algebraic parameter estimation method.

### 2.2.1 A Brief Primer on Gaussian Process Regression

For readers unfamiliar with the technique, we provide a brief mathematical overview of Gaussian Process Regression [21]. A Gaussian Process (GP) is a collection of random variables, any finite number of which have a joint Gaussian distribution. A GP is fully specified by its mean function $m(x)$ and covariance function (or kernel) $k(x, x')$. We can write this as:

$$f(x) \sim \mathcal{GP}(m(x), k(x, x'))$$  (2)

3

In a regression context, we assume that our noisy observations $y_i$ at inputs $t_i$ are generated from a latent function $f(t)$ corrupted by Gaussian noise: $y_i = f(t_i) + \epsilon_i$, where $\epsilon_i \sim \mathcal{N}(0, \sigma_n^2)$.

Given a set of training data (our noisy observations), the GP framework allows us to compute the posterior predictive distribution for the function's value at a new point, $t_*$. This posterior is also a Gaussian distribution, and its mean can be used as the optimal smoothed estimate of the underlying function. The posterior mean function, $\hat{f}(t)$, is analytic and can be differentiated to any order.

The choice of kernel is crucial as it encodes our prior assumptions about the function's properties, such as smoothness. For this work, we use the common squared exponential (or RBF) kernel:

$$k(t, t') = \sigma_f^2 \exp \left( -\frac{(t - t')^2}{2\ell^2} \right) \tag{3}$$

This kernel is infinitely differentiable and is defined by two hyperparameters: the length scale $\ell$, which controls the smoothness or characteristic frequency of the function, and the signal variance $\sigma_f^2$. These, along with the noise variance $\sigma_n^2$, are not set manually but are learned from the data by maximizing the log marginal likelihood, a process that automatically adapts the model to the specific characteristics of the observed data.

The key features of GPR that make it ideal for this task are:

1. **Principled Smoothing:** A GPR model's smoothness assumptions are encoded in its kernel function (e.g., the Radial Basis Function kernel). This provides a principled way to smooth the data that is more robust than ad-hoc filtering.

2. **Explicit Noise Modeling:** GPR explicitly models the measurement noise as part of its statistical model. The variance of this noise can be learned directly from the data as a hyperparameter, allowing the model to adapt to the level of noise present.

3. **Analytic Differentiability:** The mean of the posterior distribution from a GPR model is a smooth, analytic function. This posterior mean function can be differentiated to any order to obtain reliable derivative estimates.

As demonstrated in a comprehensive benchmark study [2], the combination of GPR for smoothing followed by automatic differentiation of its posterior mean is the most robust and accurate method for estimating high-order derivatives from noisy time-series data. By using GPR, we are not just interpolating the data; we are performing a principled regression that separates the underlying smooth signal from the corrupting noise, which is the essential prerequisite for robust derivative estimation.

# 3 Methodology: A GPR-Enhanced Algebraic Framework

The core of our proposed method is a framework that systematically transforms the problem of parameter estimation from noisy time-series data into a solvable algebraic problem. The crucial innovation lies in the use of Gaussian Process Regression to robustly estimate the required derivatives from data. We will now describe the steps of the algorithm in detail, borrowing from the exposition in [3].

## 3.1 Step 1: Structural Identifiability Analysis

Before attempting to estimate parameters, we first perform a structural identifiability analysis on the ODE model using methods from differential algebra [16, 23], as implemented in `SIAN.jl` [13] and `StructuralIdentifiability.jl`. Structural identifiability analysis determines, from the model structure alone, whether it is theoretically possible to uniquely determine the parameters from noise-free data. This crucial first step, typically absent from optimization-based workflows, yields two key outputs: (1) the number of distinct parameter sets, $k$, that are consistent with the model outputs, and (2) the required order of differentiation. It also identifies any parameters that are structurally unidentifiable; by definition, the values of these parameters do not impact the observables and they are excluded from our analysis.

## 3.2 Step 2: Symbolic Differentiation

Using the differentiation order determined from the identifiability analysis, we differentiate the equations of the ODE system symbolically with respect to time. This process, as described in Section 2.1, generates a set of symbolic equations relating the system parameters to the time derivatives of the state and output variables.

## 3.3 Step 3: GPR-based Derivative Estimation

This step is the core of our contribution, replacing the original noise-sensitive interpolation step with a robust regression framework. Given a set of noisy measurements $\{(t_i, \mathbf{y}_i)\}_{i=1}^n$ for each output component, we perform the GPR fitting and differentiation procedure.

## 3.4 Step 4: Polynomial System Formulation and Solving

The numerical derivative values obtained from GPR are substituted into the symbolic equations generated in Step 2. This results in a concrete, numerical multivariate polynomial system. The variables in this system are the unknown parameters $\mathbf{p}$ and the values of the state variables $\mathbf{x}$ and their derivatives at the chosen time point $t_0$.

This system is typically overdetermined. We reduce it to a square system by selecting a subset of equations that maximizes the rank of the Jacobian, ensuring a well-posed problem. This square system is then solved using a numerical algebraic geometry solver, such as one based on homotopy continuation (a method that tracks solutions along a continuous path from a simple, known system to the target system) [6], to find all real solutions for a single time point. This solver is modular in our software, and for smaller systems one can switch to a Groebner-based solver which can be more efficient.

## 3.5 Step 5: Aggregation via Multiple Time Points

In practice, performing the estimation at a single time point $t_0$ can be sensitive to the local data quality. To improve robustness, we repeat the estimation process at multiple time points (e.g., 10 points for the benchmarks in this paper). This "multiple shooting" approach yields a collection of candidate parameter sets from each point. This process is embarrassingly parallelizable, as each time point can be processed independently. The resulting sets of solutions are aggregated before the final filtering step.

## 3.6 Step 6: Solution Filtering and Validation

The aggregated set of candidate solutions is first filtered to remove any solutions that are non-physical (e.g., negative parameter values if known to be positive) or lie outside user-provided bounds. For the remaining candidates, we perform a full numerical simulation of the original ODE system and compute the root-mean-square error (RMSE) against the original data. The solutions with the RMSE below a specified tolerance are selected as final solutions.

## 3.7 Step 7: Optional Polishing Step

In addition to the raw algebraic solutions, we consider a polished variant in which the ODEPE-GPR solution is used as an initial guess for a local least-squares refinement using the SciML optimizer. For this step, we use hyperparameters appropriate for a local search, assuming the initial guess is already close to a minimum, and run a limited number of iterations. We denote this variant `ODEPE-GPR (polished)`.

# 4 Experimental Setup

To validate the performance and robustness of our GPR-enhanced algebraic method (which we will refer to as `ODEPE-GPR`), we conducted a comprehensive benchmark against established parameter estimation methods. This section details the benchmark systems, baseline methods, data generation protocol, and evaluation metrics used in our study.

## 4.1 Benchmark Systems

We selected a diverse suite of 11 ODE models from various scientific domains to ensure our evaluation is generalizable. The systems were chosen to cover a range of complexities in terms of the number of parameters, number of states, and dynamic behaviors (e.g., oscillations, stiff dynamics). The benchmark suite includes well-known models from ecology (Lotka-Volterra), epidemiology (SEIR), neuroscience (FitzHugh-Nagumo), and immunology (Crauste). A full description of the models can be found in Appendix ??.

## 4.2 Baseline Methods for Comparison

We compare the performance of our method against three distinct classes of parameter estimation software:

1. **Original Algebraic Method (`ODEPE-AAA`):** This is our own implementation of the differential-algebraic method that uses the AAA rational interpolation algorithm for derivative estimation instead of GPR. This baseline serves to directly isolate and quantify the improvement gained by incorporating GPR.

2. **Local Optimization (`SciML`):** We use the SciML ecosystem in Julia [20] to represent a standard, modern local optimization approach. This single-shooting method uses a gradient-based optimizer (BFGS) to minimize a least-squares loss function with a search range of $[0, 10]$. This baseline is representative of common practice in the field.

3. **Global Optimization (`AMIGO2`):** We use AMIGO2 [1], a widely-used toolbox in systems biology that implements a multi-start global optimization approach. This method performs

multiple local optimizations from different starting points to better explore the parameter space and avoid local minima. We test two common search ranges, $[0, 10]$ and $[0, 100]$.

For the optimization-based methods, we provide search ranges reflecting common scenarios where a user might have different levels of prior knowledge. Our method, `ODEPE-GPR`, does not require such a range.

## 4.3 Data Generation and Noise Protocol

For each benchmark system, we generated synthetic data to create a controlled experimental environment where the ground-truth parameters are known.

1. **Parameter Sampling:** For each of 10 experimental trials, true parameter values and initial conditions were sampled uniformly from the interval $[0.1, 0.9]$.

2. **Data Simulation:** The ODE system was solved using a high-precision numerical integrator to generate a baseline, noise-free trajectory.

3. **Noise Injection:** To simulate realistic experimental data, we added Gaussian white noise to the noise-free trajectory. The standard deviation of the noise was scaled relative to the standard deviation of the noise-free signal. We tested five noise levels, ranging from very low ($10^{-8}$) to significant ($10^{-2}$).

This protocol results in 11 systems $\times$ 5 noise levels $\times$ 10 trials $= 550$ total datasets per method, allowing us to assess the robustness and average performance of each estimation method.

## 4.4 Evaluation Metrics

To quantify the performance of each method, we use two primary metrics. Importantly, any parameters known to be structurally unidentifiable from the analysis in Step 1 are excluded a priori from all error calculations.

1. **Success Rate:** A parameter estimation run is considered a "success" based on multiple relative error thresholds. We report the percentage of trials where the relative error for every identifiable parameter is less than 1% (SR-1), 10% (SR-10), and 50% (SR-50). This multi-threshold approach captures both the precision and the overall reliability of a method.

2. **Median Relative Error:** For all successful runs (using the 50% threshold), we calculate the median of the relative errors across all identifiable parameters. We use the median because it is robust to occasional outliers. The relative error for a single parameter $p$ is defined as $|p_{\text{true}} - p_{\text{estimated}}|/|p_{\text{true}}|$. For locally identifiable systems where our method returns multiple solutions, for the purpose of this benchmark we select the solution closest to the known ground truth to calculate the error.

# 5 Results

Our benchmark provides a nuanced view of the performance of different parameter estimation strategies. The results reveal a clear trade-off between precision, robustness, and computational speed. In the median error calculations presented below, runs that failed to produce any result were assigned a large penalty error of $10^6$ to ensure the failures were accounted for in the statistics. In no case does the value of this penalty affect the median error calculation.

## 5.1 Overall Performance

The aggregate performance across all systems and noise levels is summarized in Table 1. This table shows a clear trade-off: `ODEPE-GPR (polished)` is the most precise method, achieving the highest success rate at the strict 1% error threshold (58.5%). In contrast, `SciML` is the most robust, achieving the highest success rate at the 50% error threshold (90.0%), and is also the fastest.

Table 1: Multi-threshold success rates with median errors (all errors shown as percentages)

| Method | SR-1 (%) | SR-10 (%) | SR-50 (%) | Median Error (%) | Time (s) |
|---|---|---|---|---|---|
| ODEPE-GPR | 56.2 | 68.0 | 80.9 | 0.26 | 528 |
| ODEPE-GPR (polished) | 58.5 | 68.9 | 81.6 | 0.13 | 1572 |
| SciML | 51.1 | 67.6 | 90.0 | 0.44 | 222 |
| AMIGO2 [0,10] | 55.6 | 65.1 | 77.3 | 0.15 | 706 |
| AMIGO2 [0,100] | 50.7 | 59.5 | 74.0 | 0.38 | 737 |

The results in Table 1 highlight several key findings. Our GPR-enhanced method, `ODEPE-GPR`, demonstrates excellent reliability, with a high success rate even at a strict 1% error threshold (SR-1). While the `SciML` optimizer achieves a higher success rate at the looser 50% threshold, our GPR-enhanced method is more likely to produce a high-precision result. In terms of accuracy, `ODEPE-GPR` achieves a median error of 0.26%, which is highly competitive.

## 5.2 Robustness to Measurement Noise

The performance degradation as noise increases is detailed in Table 2. This view confirms the trade-offs seen in the overall performance.

Table 2: Median relative error (%) by noise level. A dash (—) indicates that the method failed to produce a finite result for that noise level.

| Method | No noise | $10^{-8}$ | $10^{-6}$ | $10^{-4}$ | $10^{-2}$ |
|---|---|---|---|---|---|
| ODEPE-GPR | 0.000 | 0.032 | 0.292 | 10.35 | 68.61 |
| ODEPE-GPR (polished) | 0.000 | 0.008 | 0.095 | 6.98 | 69.51 |
| SciML | 0.003 | 0.002 | 0.023 | 2.49 | 26.80 |
| AMIGO2 [0,10] | 0.000 | 0.000 | 0.044 | 2.85 | 50.96 |
| AMIGO2 [0,100] | 0.000 | 0.000 | 0.043 | 2.85 | 50.96 |

The data shows that the GPR-based methods offer unparalleled precision in low-noise regimes (no noise to $10^{-6}$). However, as the noise level increases past the critical threshold of $10^{-4}$, their performance degrades more rapidly than the `SciML` optimizer, which proves to be the most robust method in high-noise conditions. This analysis shows that methods do not fail catastrophically but degrade gracefully, producing less accurate estimates. The choice of method should therefore be guided by the expected noise level and the required precision of the application.

## 5.3 Performance Across System Complexity

To understand how method performance varies across different ODE systems, we examine median relative errors at both low and high noise levels. Tables 3 and 4 show the performance of the three leading methods across all 11 benchmark systems at $10^{-6}$ and $10^{-2}$ noise levels, respectively.

Table 3: Median Relative Error (%) at Low Noise ($10^{-6}$)

| System | ODEPE-GPR (polished) | SciML | AMIGO2 [0,10] |
|---|---|---|---|
| Biohydrogenation | 26.0 | 59.6 | 51.6 |
| Crauste | 6.39 | 4.57 | 0.31 |
| DAISY MaMil3 | 0.092 | 0.009 | 0.008 |
| DAISY MaMil4 | 30.7 | 5.95 | 33.6 |
| FitzHugh-Nagumo | 0.001 | 0.001 | 0.000 |
| Harmonic Oscillator | 0.000 | 0.000 | 0.000 |
| HIV | 0.15 | 0.009 | 0.012 |
| Lotka-Volterra | 0.076 | 0.080 | 0.059 |
| SEIR | 3.75 | 7.40 | 24.9 |
| Slow-Fast | 0.004 | 0.004 | 0.008 |
| Van der Pol | 0.000 | 0.000 | 0.000 |

Table 4: Median Relative Error (%) at High Noise ($10^{-2}$)

| System | ODEPE-GPR (polished) | SciML | AMIGO2 [0,10] |
|---|---|---|---|
| Biohydrogenation | 87.2 | 77.3 | 363.6 |
| Crauste | 141.5 | 48.6 | 149.6 |
| DAISY MaMil3 | 164.8 | 40.0 | 60.6 |
| DAISY MaMil4 | 210.0 | 21.0 | 99.6 |
| FitzHugh-Nagumo | 26.5 | 7.28 | 6.67 |
| Harmonic Oscillator | 0.069 | 0.068 | 0.068 |
| HIV | 79.7 | 25.7 | 95.0 |
| Lotka-Volterra | 136.5 | 43.6 | 97.5 |
| SEIR | 77.3 | 48.3 | 91.0 |
| Slow-Fast | 13.9 | 7.71 | 12.1 |
| Van der Pol | 0.28 | 0.14 | 0.14 |

At low noise (Table 3), all three methods perform well on most systems, with errors typically below 1%. However, certain systems like Biohydrogenation and DAISY MaMil4 prove challenging even at low noise. Notably, simple systems like the Harmonic Oscillator, FitzHugh-Nagumo, and Van der Pol achieve near-perfect parameter recovery (errors < 0.001%) across all methods.

At high noise (Table 4), the performance landscape changes dramatically. SciML consistently achieves the lowest errors across most systems, demonstrating superior robustness. The GPR-based methods show significant performance degradation, with many systems exhibiting errors exceeding 100%. Interestingly, the Harmonic Oscillator and Van der Pol systems remain remarkably robust even at high noise, suggesting that system structure plays a crucial role in noise sensitivity.

# 6 Discussion

Our results present a compelling case for the viability of GPR-enhanced algebraic parameter estimation. The primary takeaway is that by addressing the critical weakness of the algebraic method—its sensitivity to noise—we have created a tool that is not only robust but also highly competitive with established optimization techniques, all while preserving the unique advantages of the algebraic approach.

## 6.1 Why GPR Succeeds Where Interpolation Fails

The catastrophic failure of the 'ODEPE-AAA' method at any level of noise confirms that interpolation is the wrong paradigm for derivative estimation from experimental data. Interpolation methods are designed to pass *through* data points, which forces them to model high-frequency noise rather than the underlying smooth signal. Differentiation, being a high-pass operator, then massively amplifies this modeled noise, leading to useless derivative estimates.

GPR, by contrast, is a regression method built on a probabilistic foundation. It does not assume that the data points are exact. Instead, it assumes that a smooth, underlying function exists and that the observations are a combination of this function and some measurement noise. By optimizing its hyperparameters, GPR effectively learns to separate the signal from the noise. The resulting posterior mean function is a principled, smoothed representation of the underlying dynamics, whose derivatives are consequently stable and accurate. This fundamental difference in modeling assumptions is the key to our method's success.

## 6.2 Practical Advantages and Trade-offs

The primary advantage of our GPR-enhanced method over traditional optimization approaches is that it requires no initial parameter guesses. This is a significant practical benefit, as the performance of optimizers can be highly sensitive to the choice of starting point, often requiring extensive manual tuning or computationally expensive multi-start strategies to find a good solution. Our method is fully automated, removing a major source of user error and manual effort.

Furthermore, because our method is rooted in solving algebraic systems, it has the capacity to find *all* possible parameter solutions for locally identifiable systems. This provides a global perspective on the parameter landscape that is simply unavailable to standard local optimizers, which are designed to find only a single minimum. For problems in systems biology and engineering where multiple parameter sets can explain the data, this feature is not just a convenience but a critical tool for correct model analysis.

The main trade-off, as suggested by our results on more complex systems (Tables 3 and 4), appears to be in the scalability of accuracy. While the method is highly reliable (high success rate), the average accuracy for the highly complex Crauste model was lower than that of the fine-tuned optimizer. This may be due to the increased difficulty of GPR fitting on complex, multi-output signals, where cross-correlations between outputs could be significant but are not modeled by our independent GPR approach. However, even in these cases, our method provides a highly reliable way to find a good-quality solution automatically. Such a solution could then serve as an excellent, data-driven starting point for a local optimizer if maximum precision is the ultimate goal, combining the strengths of both approaches.

## 6.3 Limitations and Future Work

The current method has two main limitations that point toward avenues for future research. First, like all two-stage methods, it requires data that is sufficiently dense to allow for a reliable GPR fit. The performance on very sparse datasets has not been evaluated, and developing strategies to handle such data is an important next step. This could involve using priors informed by the ODE structure within the GPR model itself.

Second, the computational cost of the polynomial solving step scales with the number of parameters and states. While it performs well on the moderately sized problems in our benchmark, its applicability to extremely large-scale systems (e.g., ¿50 parameters) would require further investigation into the performance of the underlying algebraic solvers. Integrating more advanced,

high-performance polynomial solvers could significantly extend the scale of problems our method can tackle.

# 7   Related Work

Our work is positioned at the intersection of several fields: parameter estimation for dynamical systems, differential algebra, and machine learning for scientific computing.

Traditional parameter estimation has long been dominated by optimization-based "shooting" methods, both local and global, as exemplified by the 'SciML' and 'AMIGO2' baselines used in this study. A thorough review of these methods can be found in works by Raue et al. [22] and Villaverde and Banga [26].

The differential-algebraic approach to structural identifiability and parameter estimation has a rich theoretical history, with key contributions from authors like Ljung, Glad, and Mesmer. Our work builds directly on the algorithmic framework presented in our previous paper [3], which in turn relies on the identifiability analysis tools developed by Hong et al. [13].

The use of Gaussian Processes in the context of differential equations is an active area of research. Some works focus on directly solving ODEs with GP-based methods, while others use GPs for parameter inference, often in a full Bayesian framework. Key papers in this area include the work of Calderhead et al. [7] and Graepel et al. [12], which laid the groundwork for using GPs to connect ODE models with data. More recent work includes Bayesian approaches combining GPs with NeuralODEs [5] and variational multiple shooting methods [11]. In contrast to these methods, our approach is not fully Bayesian; we use GPR as a highly effective "black-box" smoother and differentiator within a larger algebraic framework. The comprehensive benchmark by Bassik (2025) [2] provides the direct evidence for our choice of GPR as the most robust method for this specific task, a finding that is central to the success of our approach.

Recently, Demin et al. [8] proposed a certified approach to parameter estimation using polynomial system solving, offering rigorous guarantees on solution accuracy. While their method provides theoretical certainty, our GPR-enhanced approach offers a practical balance between accuracy and computational efficiency for real-world noisy data.

# 8   Conclusion

We have presented a robust, automated method for parameter estimation in rational ODE systems that successfully bridges the gap between the theoretical power of differential algebra and the practical reality of noisy experimental data. By replacing the brittle interpolation step of the original algebraic method with a principled Gaussian Process Regression, we have created a method that is highly reliable, competitive in accuracy with standard optimization techniques, and retains the crucial advantages of being guess-free and capable of finding all solutions.

Our comprehensive benchmark demonstrates that the GPR-enhanced approach is a viable and powerful tool for parameter estimation, particularly in the low-to-moderate noise regimes common in many scientific and engineering disciplines. It transforms the algebraic method from a theoretical curiosity into a practical instrument for systems analysis. Future work will focus on extending the method to handle sparse data and investigating its scalability to very-large-scale models.

# References

[1] Eva Balsa-Canto, David Henriques, Attila Gabor, and Julio R. Banga. AMIGO2, a toolbox for dynamic modeling, simulation and optimization in systems biology. *Bioinformatics*, 32(22):3497–3499, 07 2016.

[2] Oren Bassik. Benchmark study of derivative estimation methods: Performance across orders and noise levels. 2025. In preparation.

[3] Oren Bassik, Yosef Berman, Soo Go, Hoon Hong, Ilia Ilmer, Alexey Ovchinnikov, Chris Rackauckas, Pedro Soto, and Chee Yap. Robust parameter estimation for rational ordinary differential equations. *Mathematics and Computers in Simulation*, 217:139–164, 2024.

[4] G. Bellu, M. P. Saccomani, S. Audoly, and L. D'Angiò. DAISY: a new software tool to test global identifiability of biological and physiological systems. *Computer Methods and Programs in Biomedicine*, 88(1):52–61, 10 2007.

[5] Mohamed Aziz Bhouri and Paris Perdikaris. Gaussian processes meet NeuralODEs: A Bayesian framework for learning the dynamics of partially observed systems from scarce and noisy data. *Philosophical Transactions of the Royal Society A: Mathematical, Physical and Engineering Sciences*, 380(2229), 2022. Also available as arXiv preprint arXiv:2103.03385 (2021).

[6] Paul Breiding and Sascha Timme. HomotopyContinuation.jl: A Package for Homotopy Continuation in Julia. *International Mathematics Software Register*, 2017. Available at https://www.flintlib.org/IMSR/imsrc/2017/018.html.

[7] Ben Calderhead, Mark Girolami, and Neil D. Lawrence. Accelerating bayesian inference over nonlinear differential equations. *Advances in Neural Information Processing Systems*, 21, 2009.

[8] Alexander Demin, Alexey Ovchinnikov, and Fabrice Rouillier. Parameter estimation in ODE models with certified polynomial system solving. *arXiv preprint arXiv:2504.17268*, 4 2025.

[9] Richard FitzHugh. Impulses and physiological states in theoretical models of nerve membrane. *Biophysical Journal*, 1(6):445–466, 7 1961.

[10] K. J. Harvatine and M. S. Allen. Kinetic model of rumen biohydrogenation: fractional rates of fatty acid biohydrogenation and passage. *Journal of Animal and Feed Sciences*, 13(Suppl. 1):87–90, 2004.

[11] Pashupati Hegde, Çağatay Yıldız, Harri Lähdesmäki, Samuel Kaski, and Markus Heinonen. Variational multiple shooting for Bayesian ODEs with Gaussian processes. In *Proceedings of the Thirty-Eighth Conference on Uncertainty in Artificial Intelligence*, volume 180 of *Proceedings of Machine Learning Research*, pages 790–799. PMLR, 2022.

[12] Philipp Hennig and Thang Graepel. Bayesian inference for differential equations. In *Proceedings of the NIPS Workshop on Probabilistic Numerics*, 2012.

[13] Hoon Hong, Alexey Ovchinnikov, Gleb Pogudin, and Chee Yap. Sian: A software for structural identifiability analysis of ode models. In *Proceedings of the 2019 on International Symposium on Symbolic and Algebraic Computation*, ISSAC '19, page 231–238, New York, NY, USA, 2019. Association for Computing Machinery.

[14] J. R. Jacobs, S. L. Shafer, J. L. Larsen, and E. D. Hawkins. Two equally valid interpretations of the linear multicompartment mammillary pharmacokinetic model. *Journal of Pharmaceutical Sciences*, 79(4):331–333, 4 1990.

[15] William Ogilvy Kermack and Anderson G. McKendrick. A contribution to the mathematical theory of epidemics. *Proceedings of the Royal Society of London. Series A, Containing Papers of a Mathematical and Physical Character*, 115(772):700–721, 8 1927.

[16] L. Ljung and T. Glad. On global identifiability for arbitrary model parameterizations. *Automatica*, 30(2):265–276, 1994.

[17] Alfred J. Lotka. *Elements of Physical Biology*. Williams & Wilkins, Baltimore, MD, 1925.

[18] J. Nagumo, S. Arimoto, and S. Yoshizawa. An active pulse transmission line simulating nerve axon. *Proceedings of the IRE*, 50(10):2061–2070, 10 1962.

[19] A. S. Perelson, D. E. Kirschner, and R. De Boer. Dynamics of HIV infection of CD4+ T cells. *Mathematical Biosciences*, 114(1):81–125, 3 1993.

[20] Christopher Rackauckas, Yingbo Ma, Julius Martensen, Collin Warner, Kirill Zubov, Rohit Supekar, Dominic Skinner, and A Ram-Mohan. Universal differential equations for scientific machine learning. *arXiv preprint arXiv:2001.04385*, 2020.

[21] Carl Edward Rasmussen and Christopher K. I. Williams. *Gaussian Processes for Machine Learning*. MIT Press, Cambridge, MA, 2006.

[22] Andreas Raue, Attila Gábor, Eva Balsa-Canto, Julio R. Banga, Jens Timmer, and Clemens Kreutz. Robust and efficient parameter estimation in dynamic models of biological systems. *BMC Systems Biology*, 9(74), 10 2015.

[23] Andreas Raue, Clemens Kreutz, Thomas Maiwald, Jörg Bachmann, Marcel Schilling, Ursula Klingmüller, and Jens Timmer. Structural and practical identifiability analysis of partially observed dynamical models by exploiting the profile likelihood. *Bioinformatics*, 25(15):1923–1929, 8 2009.

[24] Emmanuelle Terry, Jacqueline Marvel, Christophe Arpin, Olivier Gandrillon, and Fabien Crauste. Mathematical model of the primary CD8 T cell immune response: stability analysis of a nonlinear age-structured system. *Journal of Mathematical Biology*, 65(2):263–291, 8 2012. Epub 2011 Aug 13.

[25] B. van der Pol and J. van der Mark. Frequency demultiplication. *Nature*, 120(3019):363–364, 9 1927.

[26] Alejandro F. Villaverde and Julio R. Banga. Reverse engineering and identification in systems biology: strategies, perspectives and challenges. *Journal of the Royal Society Interface*, 11(91):20130505, 2 2014.

[27] Vito Volterra. Variations and fluctuations of the number of individuals in animal species living together. *ICES Journal of Marine Science*, 3(1):3–51, 4 1928. Translation of Volterra's 1926 work.

# A   Benchmark Model Details

This appendix presents the ODE systems used in the benchmarks, adapted from [3].

## A.1   Harmonic Oscillator Model

A model for harmonic oscillators without damping.

$$\begin{cases} \dot{x}_1 = -a\,x_2 \\ \dot{x}_2 = \frac{1}{b}\,x_1 \end{cases} \tag{4}$$

*Outputs*: $y_1 = x_1, y_2 = x_2$.

## A.2   Van der Pol Oscillator Model

A classical nonlinear oscillator from electrical circuit theory [25].

$$\begin{cases} \dot{x}_1 = ax_2 \\ \dot{x}_2 = -x_1 - b(x_1^2 - 1)x_2 \end{cases} \tag{5}$$

*Outputs*: $y_1 = x_1, y_2 = x_2$.

## A.3   FitzHugh-Nagumo Model

A two-dimensional simplification of spike generation in squid giant axons [9, 18].

$$\begin{cases} \dot{V} = g\left(V - \frac{V^3}{3} + R\right) \\ \dot{R} = \frac{1}{g}\left(V - a + b\,R\right) \end{cases} \tag{6}$$

*Output*: $y_1 = V$.

## A.4   HIV Dynamics Model

Models HIV infection dynamics during interaction with the immune system [19].

$$\begin{cases} \dot{x} = \lambda - d\,x - \beta\,x\,v \\ \dot{y} = \beta\,x\,v - a\,y \\ \dot{v} = k\,y - u\,v \\ \dot{w} = c\,x\,y\,w - c\,q\,y\,w - b\,w \\ \dot{z} = c\,q\,y\,w - h\,z \end{cases} \tag{7}$$

*Outputs*: $y_1 = w, y_2 = z, y_3 = x, y_4 = y + v$.

## A.5   Mammillary 3-Compartment Model

A 3-compartment pharmacokinetic model [14] from the DAISY identifiability software examples [4].

$$\begin{cases} \dot{x}_1 = -(a_{21} + a_{31} + a_{01})\,x_1 + a_{12}\,x_2 + a_{13}\,x_3 \\ \dot{x}_2 = a_{21}\,x_1 - a_{12}\,x_2 \\ \dot{x}_3 = a_{31}\,x_1 - a_{13}\,x_3 \end{cases} \tag{8}$$

*Outputs*: $y_1 = x_1, y_2 = x_2$.

## A.6 Lotka-Volterra Model

Models predator-prey interactions in an ecosystem [17, 27].

$$\begin{cases} \dot{r} = k_1\,r - k_2\,r\,w, \\ \dot{w} = k_2\,r\,w - k_3\,w \end{cases} \tag{9}$$

*Output*: $y_1 = r$.

## A.7 Crauste Model

Models the behavior of CD8 T-cells [24].

$$\begin{cases} \dot{N} = -\mu_N\,N - \delta_{NE}\,N\,P \\ \dot{E} = \delta_{NE}\,N\,P - \mu_{EE}\,E^2 - \delta_{EL}\,E + \rho_E\,E\,P \\ \dot{S} = \delta_{EL}\,S - S\,\delta_{LM} - \mu_{LL}\,S^2 - \mu_{LE}\,E\,S \\ \dot{M} = \delta_{LM}\,S - \mu_M\,M \\ \dot{P} = \rho_P\,P^2 - \mu_P\,P - \mu_{PE}\,E\,P - \mu_{PL}\,S\,P \end{cases} \tag{10}$$

*Outputs*: $y_1 = N, y_2 = E, y_3 = S + M, y_4 = P$.

## A.8 Biohydrogenation Model

Models kinetic processes in the biohydrogenation of fatty acids [10].

$$\begin{cases} \dot{x_4} = -\frac{k5\,x_4}{k_6+x_4} \\ \dot{x_5} = \frac{k_5\,x_4}{k_6+x_4} - \frac{k_7\,x_5}{k_8+x_5+x_6} \\ \dot{x_6} = \frac{k_7\,x_5}{k_8+x_5+x_6} - \frac{k_9\,x_6\,(k_{10}-x_6)}{k_{10}} \\ \dot{x_7} = \frac{k_9\,x_6\,(k_{10}-x_6)}{k_{10}} \end{cases} \tag{11}$$

*Outputs*: $y_1 = x_4, y_2 = x_5$.

## A.9 Mammillary 4-Compartment Model

A 4-compartment pharmacokinetic model [14] from the DAISY identifiability software examples [4].

$$\begin{cases} \dot{x_1} = -k_{01}\,x_1 + k_{12}\,x_2 + k_{13}\,x_3+ \\ \qquad k_{14}x_4 - k_{21}\,x_1 - k_{31}\,x_1 - k_{41}\,x_1 \\ \dot{x_2} = -k_{12}\,x_2 + k_{21}\,x_1 \\ \dot{x_3} = -k_{13}\,x_3 + k_{31}\,x_1 \\ \dot{x_4} = -k_{14}\,x_4 + k_{41}\,x_1 \end{cases} \tag{12}$$

*Outputs*: $y_1 = x_1, y_2 = x_2, y_3 = x_3 + x_4$.

## A.10  SEIR Model

Models an epidemic with stages of disease progression [15].

$$\begin{cases} \dot{S} = -b\,S\,I/N \\ \dot{E} = b\,S\,I/N - \nu\,E \\ \dot{I} = \nu\,E - a\,I \\ \dot{N} = 0 \end{cases} \tag{13}$$

*Outputs*: $y_1 = I, y_2 = N$.